Journal of Materials Chemistry A

ROYAL SOCIETY OF CHEMISTRY

PAPER

View Article Online
View Journal

Check for updates

Cite this: DOI: 10.1039/d6ta00383d

Approaching the reactivity of anions in battery electrolytes *via* conceptual density functional theory

Ervin Rems, [ab] Matej Huš [*cd] and Robert Dominko [*abe]

The practical deployment of batteries with superior energy and power densities is, among other factors, prohibited by the lack of suitable electrolyte formulations. While first-principles design promises accelerated discovery of practical battery electrolytes, its high computational cost limits the chemical space that can be analysed through screening. Herein, we show a computationally inexpensive approach, using descriptors within the framework of conceptual density functional theory, that can provide valuable insights into the reactivity of battery electrolyte components. By focusing on anions in liquid electrolytes for which abundant experimental data is available for benchmarking, we explore several descriptors against key experimental observables for a series of salts ($LiPF_6$, $LiBF_4$, LiTFSI, LiDFOB, LiTDI). We show that the descriptors evaluated for single species can provide insights consistent with those obtained from experiments or more complex models, while maintaining a favourable computational cost. This establishes conceptual density functional theory as a promising tool for high-throughput screening of electrolyte components (salts, solvents, diluents, additives).

Received 14th January 2026
Accepted 19th February 2026

DOI: 10.1039/d6ta00383d

rsc.li/materials-a

Open Access Article. Published on 19 February 2026. Downloaded on 4/7/2026 12:08:39 AM.
This article is licensed under a Creative Commons Attribution 3.0 Unported Licence.

1. Introduction

Lithium-ion batteries have revolutionized energy storage, enabling the rapid expansion of portable electronics and electric vehicles.[1] However, for further electrification of society, an additional increase in the energy density of Li batteries is crucial, expanding their range of applications and optimizing the cost.[2] Three main directions to increase Li battery energy density are (i) decreasing the battery mass by replacing a negative graphite electrode with metallic Li,[3] (ii) increasing battery output voltage by employing high-voltage positive electrode materials,[4] and (iii) the use of positive electrode materials with high specific capacity.[5] A major challenge of these approaches is their incompatibility with conventional Li-ion battery electrolytes, mainly due to Li dendrite growth and electrolyte degradation.[6] New electrolytes are needed for advancing application-relevant battery technologies, which can be proposed by systematic screening and rational design.[7]

Leveraging *in silico* screening approaches for battery electrolyte discovery is a promising avenue to accelerate the search across the extensive chemical space of electrolyte components.[8] Hitherto reported studies typically rely on density functional theory (DFT) calculations,[8,9] classical molecular dynamics (MD) simulations,[10,11] machine learning of experimental data,[12,13] or a combination of these methods.[14–16] However, these approaches come with important drawbacks: classical MD simulations depend on the availability of experimentally validated force–field parameters[17] with limited transferability, reducing the predictive power for experimentally unexplored formulations. Similarly, the performance of machine learning models remains limited to analogous formulations, performing poorly for compositions that differ significantly from the training set.[18,19] While DFT can be readily applied to new and experimentally unexplored chemical systems, the computational cost of quantum chemical calculations presents a practical bottleneck that severely limits the searchable chemical space. Indeed, advances in DFT-based approaches that would allow screening more diverse chemical spaces and, at the same time, yield experimentally relevant descriptors have been identified as a priority research direction in computational electrolyte design.[20]

As a promising remedy, we turn to conceptual DFT, which focuses on the extraction of chemically relevant concepts and principles from DFT.[21,22] While conceptual DFT has long established itself as a standard methodology in theoretical organic chemistry,[23] it has received surprisingly limited attention in the context of battery electrolytes,[24–29] and has not been systematically compared to experimental observables across a range of chemical compositions.

[a]Department of Materials Chemistry, National Institute of Chemistry, Hajdrihova 19, SI-1001 Ljubljana, Slovenia. E-mail: robert.dominko@ki.si
[b]Faculty of Chemistry and Chemical Technology, University of Ljubljana, Večna pot 113, SI-1000 Ljubljana, Slovenia
[c]Department of Catalysis and Chemical Reaction Engineering, National Institute of Chemistry, Hajdrihova 19, SI-1001 Ljubljana, Slovenia. E-mail: matej.hus@ki.si
[d]Association for Technical Culture of Slovenia (ZOTKS), Zaloška 65, SI-1000 Ljubljana, Slovenia
[e]ALISTORE - European Research Institute, FR CNRS 3104, 80039 Amiens Cedex, France

Open Access Article. Published on 19 February 2026. Downloaded on 4/7/2026 12:08:39 AM. This article is licensed under a Creative Commons Attribution 3.0 Unported Licence.

Here, we show that descriptors within the framework of conceptual DFT can provide valuable insights into the (electro) chemical properties of battery electrolytes at a very moderate computational cost. As an example, we focus on anions as they strongly influence electrolyte structure, transport properties, and electrochemical behaviour.[30–33] We assess the effect of anions on the electrochemical stability of the electrolyte, the mechanism of their oxidative/reductive anion decomposition, and the interaction of anions with nucleophiles/electrophiles, by focusing on electrolytes based on $LiPF_6$, $LiBF_4$, lithium bis(trifluoromethylsulfonyl)azanide (LiTFSI), lithium difluoro(oxalato)borate (LiDFOB) and lithium 2-trifluoromethyl-4,5-dicyanoimidazole (LiTDI) salts (structural formulae of the corresponding anions are shown in Fig. 1a). This set of anions was chosen to capture the chemical diversity (size, charge delocalization, functional groups) of battery electrolyte salts, while remaining small enough to allow direct comparison with previous experimental studies and costly high-level calculations rather than screen a vast theoretical configurational space. In essence, this is a conceptual study rather than a screening endeavor.

2. Computational method

First-principles calculations were performed at the DFT level, employing a long-range- and dispersion-corrected hybrid functional ωB97X-D.[34] Molecular geometries were optimized within the def2-TZVPD basis set,[35,36] while the def2-QZVPD basis set[36,37] was employed for single-point calculations. The DFT calculations were performed using Gaussian 16 (ES64L-G16RevC.02).[38] Basis sets were obtained through Basis Set Exchange (BSE).[39] Pymatgen[40] and Multiwfn[41] were used to handle input/output files. Visual Molecular Dynamics (VMD)[42] was used for visualization. The convergence criterion for geometry optimization was set using the `Opt=tight` keyword to apply the following convergence thresholds: maximum force $< 1.5 \times 10^{-5}\ E_h a_0^{-1}$, root mean square (RMS) force $< 1.0 \times 10^{-5}\ E_h a_0^{-1}$, maximum step $< 6.0 \times 10^{-5}$ Å, and RMS step $< 4.0 \cdot 10^{-5}$ Å. Vibrational analysis was performed to verify the minima of the potential energy surface through the absence of vibrational modes with imaginary frequencies. In models that include implicit solvation, the EC : EMC 3 : 7 blend ($\varepsilon = 18.5$)[43] was mimicked with the solvent parameters of acetone ($\varepsilon = 20.5$), which is deemed an adequate approximation.[44,45] Li^+-anion association strength is reported as the opposite of the Li^+-anion binding energy ΔE. In the calculation of bond dissociation energies, the geometries of all species were optimized.

3. Results and discussion

A key parameter limiting the output voltage of a battery cell is the electrochemical stability window (ESW) of the electrolyte,[46] *i.e.*, the range in volts between its limits of oxidative and reductive decomposition. Therefore, we first focus on the effect

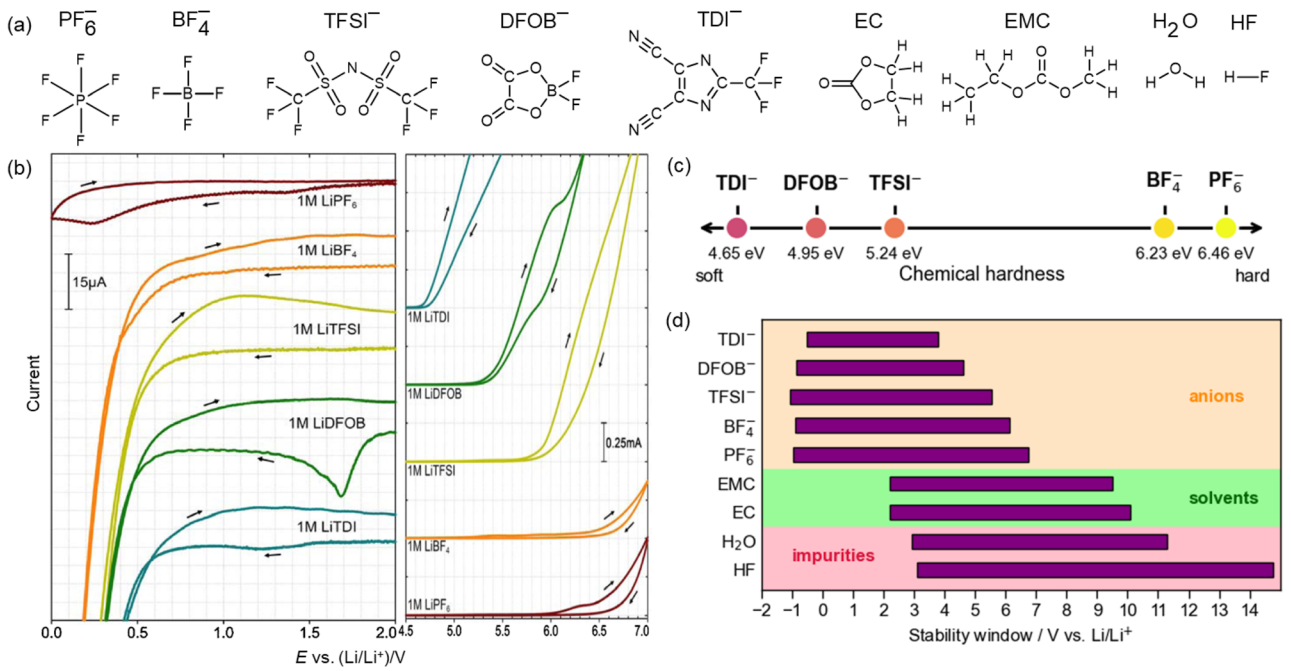

Fig. 1 Stability of electrolyte components explored in this work. (a) Structural formulae of PF_6^-, BF_4^-, bis(trifluoromethanesulfonyl)azanide ($TFSI^-$), difluoro(oxalato)borate ($DFOB^-$), 4,5-dicyano-2-(trifluoromethyl)imidazole-1-ide (TDI^-) salt anions, ethylene carbonate (EC) and ethyl methyl carbonate (EMC) solvent molecules, and H_2O and HF molecules as common impurities. (b) Experimental reduction (left) and oxidation (right) cyclic voltammetry curves of various 1 M salt in EC : EMC (3 : 7 wt%) solvent mixtures. (This panel is reprinted from Delp *et al.*[48] with permission from Elsevier.). (c) Chemical hardness of the investigated anions, without accounting for solvent. (d) Stability windows of investigated anions, solvents, and impurities. Oxidation limit is determined as the ionization potential of the corresponding species, whereas reduction limit is determined as the electronic affinity of the species-Li^+ cluster.

 This journal is © The Royal Society of Chemistry 2026

Open Access Article. Published on 19 February 2026. Downloaded on 4/7/2026 12:08:39 AM.
This article is licensed under a Creative Commons Attribution 3.0 Unported Licence.

of the Li salt by comparing the ESW of 1 M solutions of the five salts in ethylene carbonate (EC): ethyl methyl carbonate (EMC) (3 : 7 weight ratio), a typical solvent blend and salt concentration used in commercial Li-ion batteries.[47] Delp *et al.* experimentally investigated the ESWs of these systems by cyclic voltammetry (CV) measurements using a glassy carbon working electrode (Fig. 1b).[48] Experimentally, ESWs of electrolytes (disregarding small irreversible peaks that likely originate from impurities) widen, as follows: LiTDI < LiDFOB < LiTFSI < $LiBF_4$ < $LiPF_6$.

We begin by exploring a simple descriptor of global anion stability, the absolute hardness η.[49] It is defined as the second derivative of energy with respect to the number of electrons:

$$\eta = \frac{1}{2}\left(\frac{\partial^2 E}{\partial N^2}\right)_Z \doteq \frac{1}{2}(E_{N+1} + E_{N-1} - 2E_N) \quad (1)$$

Here, E indicates the energy, N the number of electrons, and Z the number of nucleons (*i.e.*, emphasizing the fixed atomic nucleus). Absolute hardness was introduced as a quantitative extension of the qualitative hard and soft acids and bases (HSAB) theory.[50] In this context, anions of battery electrolytes can be viewed as HSAB bases, with η quantifying their hardness/softness character. We rank the five anions from soft to hard based on their absolute hardness in the gas phase in Fig. 1c. Remarkably, the ranking of anions based on a simple descriptor of η qualitatively aligns with the experimental ESW of corresponding 1 M EC/EMC electrolytes. This supports the intuitive correlation between the electronic stabilization of an anion (η) and the ESW of the corresponding electrolytes. This holds as long as the stability is governed by the anion rather than by solvent or impurity oxidation, and the modeling of anions in the gas phase emphasizes intrinsic anion properties without the influence of the solvent. Nevertheless, we recover the same qualitative trend if we include the implicit solvation of anions *via* the integral-equation-formalism polarizable continuum model (IEF-PCM)[51] or the solvation model based on the solute electron density (SMD)[52] (Table S1). When accounting for solvent, all anions appear softer (0.9–2.0 eV) but their relative ordering remains unchanged. Similarly, Jaramillo *et al.* show that solvation effects stabilize anions and destabilize cations in terms of η. While implicit solvation is sufficient for qualitative trends, explicit solvation is required to achieve a quantitative agreement with experiment.[53]

The experimental determination of ESW is limited by the potentials at which reduction and oxidation of the electrolyte occur. While η provides a valuable approximation, it is more rigorous to address oxidation and reduction separately. To shed light on the species and effects limiting the ESW, we separately investigate the five anions, both solvent molecules, and the two common impurities: H_2O and HF. Trace amounts of both impurities are known to heavily impact the electrolyte (electro) chemistry.[54–56] Trace H_2O is always present in organic solvents, while HF is formed *via* the hydrolysis of PF_6^- anions.[57] We approximate the stability window based on the vertical ionization potential of the species and the vertical electronic affinity of the Li^+-species pair:

$$IP_{Li/Li^+} = \frac{(E_{N-1} - E_N)}{e_0} - 1.4\ V \quad (2)$$

$$EA_{Li/Li^+} = -\frac{(E_{N+1} - E_N)}{e_0} - 1.4\ V \quad (3)$$

where e_0 is the elementary charge and 1.4 V represents a conversion constant from the absolute potential scale[58] to the Li/Li^+ reference. In accordance with previous reports, EA is reported for Li^+-species pairs.[45,59]

The stability windows in the gas phase are shown in Fig. 1d. The trend of anion $IP^+_{Li/Li}$ agrees with the experimentally determined oxidative stability of the corresponding electrolytes. On the other hand, anion $EA^+_{Li/Li}$ has values well below those of the solvent or the impurities. This suggests anion-limited oxidative stability and impurity- and solvent-limited reductive stability.

Thus, we focus on anion and solvent oxidation by comparing the vertical IP in the gas phase with the adiabatic IP in the implicit solvent (Fig. 2a). The anion ordering by the experimental oxidative stability (Fig. 1b) aligns well with the ordering of vertical IP in the gas phase. Still, these results cannot explain the comparable experimental oxidative stability of $LiBF_4$ and $LiPF_6$ electrolytes. Considering adiabatic IP in the implicit solvent, the IP of EMC and EC drops below those of BF_4^- and

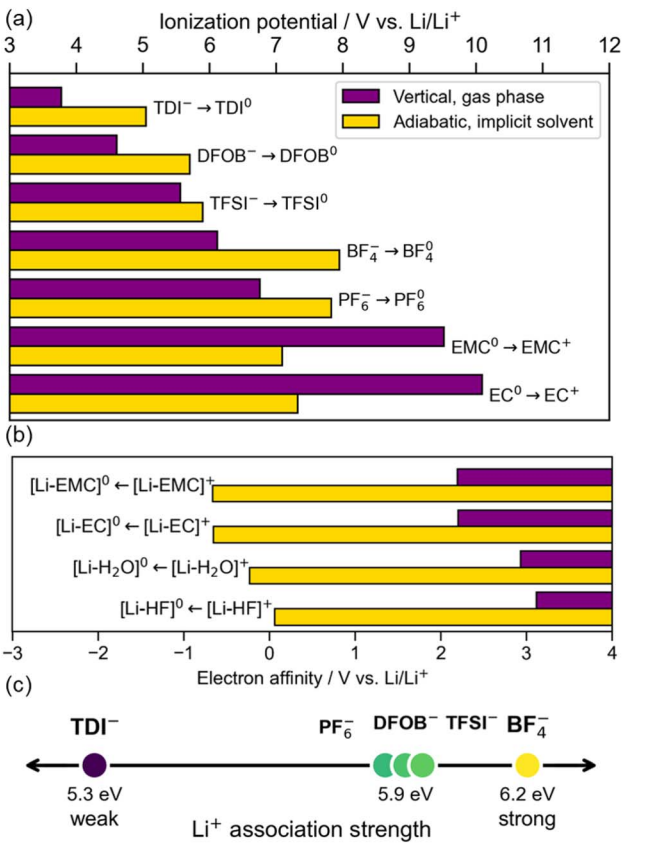

Fig. 2 Redox properties of investigated species: (a) ionization potentials (IP) for solvent molecules and anions. Vertical IP in the gas phase and adiabatic IP in the implicit solvent are shown in purple and gold, respectively. (b) Electron affinity for Li^+-solvent and Li^+-impurity pairs. (c) Li^+–anion association strength for investigated anions.

Open Access Article. Published on 19 February 2026. Downloaded on 4/7/2026 12:08:39 AM.
This article is licensed under a Creative Commons Attribution 3.0 Unported Licence.

PF_6^-, pointing to solvent-limited oxidative stability in the case of $LiBF_4$ and $LiPF_6$. This behavior agrees with an earlier report on reduced, solvent-dependent oxidative stability of systems with small difference between IP of anion and solvent[60] – as for BF_4^- and PF_6^- in the present case.

Similarly, we compare EA (electron affinity) of Li^+-solvent and Li^+-impurity pairs in Fig. 2b EAs of Li^+-anion pairs are not shown here as they are substantially lower (Fig. 1d). Despite significant quantitative differences between vertical (gas phase) and adiabatic (implicit solvent) EA, the EA increases, as follows: EMC ≈ EC < H_2O < HF. The EC < H_2O < HF ordering agrees with experimental reduction potentials.[54,55] For $LiPF_6$-based electrolytes, this suggests that anode passivation proceeds *via* sequential reduction of HF and H_2O impurities, followed by solvent reduction. This could explain the extended reductive stability of the $LiPF_6$-based electrolyte and agrees with the seminal work of Peled *et al.*, proposing a LiF-dominated inner solid electrolyte interphase (SEI), Li_2O/LiOH-dominated intermediate SEI, and organic outer SEI.[61]

Let us explore other salts beyond $LiPF_6$. The EA for Li^+-$anion^-$ species (Fig. 1d) cannot explain the differences in experimental reductive stability (Fig. 1b). Interestingly, the reductive stability does correlate with the anion association strength (Fig. 2c, SI Discussion 1 and Table S2): the stronger the ionic association, the stronger the reductive stability. We hypothesize this could be related to a higher population of contact ion pairs and ionic aggregates in electrolytes with strongly associating anions, given the tendency for ion-pair formation in EC : EMC-based electrolytes.[62] This explanation is analogous to the reasoning behind the improved reductive stability of super-concentrated electrolytes, *i.e.*, the significant population of contact ion pairs and aggregates tends to shift the reduction from solvent molecules to anions,[63] which have lower EA.Anions not only contribute to the electrolyte ESW, but can also modulate the composition of the SEI and cathode electrolyte interphase (CEI).[30,32,64] A rational design of anion-derived interphases depends on the understanding of the underlying anion decomposition mechanisms. This motivates us to explore how the electronic structure of anions responds to the extraction and addition of electrons, mimicking oxidation and reduction, respectively. This response can be characterized *via* the Fukui function $f(\vec{r})$:[65]

$$f(\vec{r}) = \left(\frac{\partial \rho(\vec{r})}{\partial N}\right)_Z \tag{4}$$

where $\rho(\vec{r})$ is the electron density. Given the discontinuity of $\rho(\vec{r})$ with respect to N,[66] it is meaningful to define the oxidative Fukui function $f^-(\vec{r})$ and the reductive Fukui function $f^+(\vec{r})$, and approximate them *via* finite differences:

$$f^-(\vec{r}) \doteq \rho_{\text{anion}}(\vec{r}) - \rho_{\text{neutral}}(\vec{r}) \tag{5}$$

$$f^+(\vec{r}) \doteq \rho_{\text{dianion}}(\vec{r}) - \rho_{\text{anion}}(\vec{r}) \tag{6}$$

where $\rho_{\text{anion}}(\vec{r})$, $\rho_{\text{neutral}}(\vec{r})$ and $\rho_{\text{dianion}}(\vec{r})$ are electron densities of the anion, neutral radical and dianion radical, respectively.

The oxidative/reductive Fukui functions for $DFOB^-$, $TFSI^-$, and TDI^- anions are illustrated in Fig. 3a (isosurface values are provided in Table S3, while in Fig. S1 we separately show positive and negative isosurfaces). The Fukui functions are evaluated in the IEF-PCM implicit solvent, except for f^+ of $DFOB^-$,

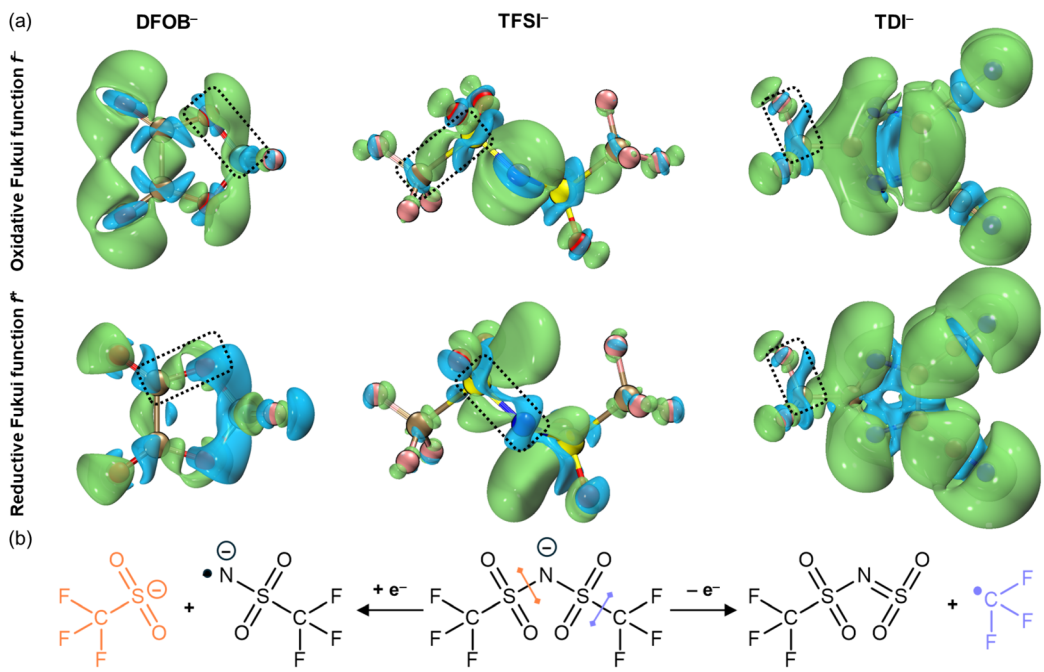

Fig. 3 Response of the anions to oxidative/reductive perturbation. (a) Oxidative (top) and reductive (bottom) real-space Fukui functions for $DFOB^-$, $TFSI^-$, and TDI^- anions. For clarity, only the positive isosurface is shown. B, C, F, N, O, S atoms are shown in pink, tan, cyan, blue, red, and yellow, respectively. (b) Proposed mechanism of the initial stage of reductive and oxidative decomposition of $TFSI^-$ anion based on bond dissociation energetics.

 This journal is © The Royal Society of Chemistry 2026

Open Access Article. Published on 19 February 2026. Downloaded on 4/7/2026 12:08:39 AM.
This article is licensed under a Creative Commons Attribution 3.0 Unported Licence.

which is evaluated in the gas phase (the corresponding IEF-PCM f^+ is shown in Fig. S2). The Fukui functions of BF_4^- and PF_6^- are not reported due to the degeneracy of their frontier molecular orbitals (see SI Discussion 2).

We first focus on the electrochemical decomposition of $DFOB^-$, an important additive in high-voltage Li-ion batteries.[67] The oxidative Fukui function f^- changes its sign along the B–O bond, suggesting its cleavage under oxidizing conditions. Indeed, the cleavage of the B–O bond has been proposed several times[68–71] as the initial stage of oxidative $DFOB^-$ decomposition, leading to a favorable passivation of the positive electrode *via* CEI formation.[72] The characterization of reductive decomposition is experimentally more challenging, as it competes with the solvent reduction,[72] which is typically more favoured (*vide supra*). However, recent *ab initio* molecular dynamics (AIMD) simulations identified the C–O(cycle) and B–F cleavage as drivers of reductive decomposition of $DFOB^-$ in a polyethylene oxide matrix on Li(100).[73] This is in line with the reductive Fukui function f^+, which points to the reductive C–O(cycle) cleavage. Henceforth, we refer to a chemical bond along which the oxidative or reductive Fukui function changes its sign as the bond of the oxidative Fukui inversion or the bond of the reductive Fukui inversion.

In $TFSI^-$, the bonds of oxidative and reductive Fukui inversion are S–C and N–S, respectively. We complement these results by evaluating the bond-breaking energetics upon electron attachment/removal (Table S4), which support C–S-cleavage-driven oxidative $TFSI^-$ decomposition and reductive decomposition *via* breaking of the N–S (Fig. 3b). Previously, the oxidative decomposition was attributed to the S–C cleavage in an organic battery electrolyte[74] and to the N–S cleavage in WiS.[75] On the other hand, studies on the reduction of $TFSI^-$-containing ionic liquids[76,77] and ether-based battery electrolyte[78] suggest a reductive decomposition *via* the N– S cleavage, while the C– F cleavage was proposed for the LiTFSI WiS electrolytes.[75,79] The oxidative/reductive Fukui inversions adequately point to breaking-prone chemical bonds, as evidenced from the agreement with the bond-breaking energetics and most previous reports.

Bond dissociation energies for TDI^- suggest the formation of fluorine radicals and fluoride anions under oxidative and reductive conditions, respectively (Table S5). The corresponding Fukui functions also point to the possibility of C–F bond breaking in both cases. We note that Fukui functions could also point to ring opening, while bond dissociation energetics suggest that this mechanism is less favorable. Previous reports have also reported the decomposition of TDI^- *via* the cleavage of the C–F bond.[80,81]

Noteworthily, Fukui function may fail to predict the correct product under kinetically controlled ambident reactivity.[82] In anionic systems with significant delocalization error, analytical evaluation of the Fukui function was shown to perform better than the finite-difference approximation.[83] Overall, while Fukui functions do provide important insights into species response to oxidative/reductive perturbation, we believe they should be interpreted with care and complemented by other methods.Another important aspect of electrolyte reactivity is their

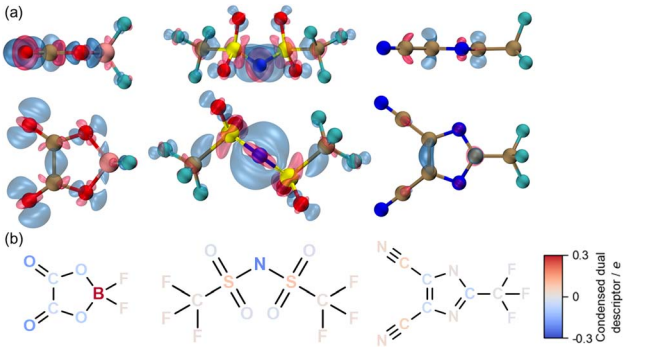

Fig. 4 Local nucleophilicity and electrophilicity of $DFOB^-$, $TFSI^-$, and TDI^- anions identified *via* dual descriptor. (a) Positive (red) and negative (blue) isosurfaces of the dual descriptor. Colour code for atoms is the same as in Fig. 3a. (b) Structural formulae of anions with atoms color based on the value of the condensed dual descriptor.

tendency for speciation with nucleophilic and electrophilic species. For example, a nucleophilic attack of H^+ on EC triggers a chemical cascade that compromises all battery components.[84] Keeping the focus on the three anions, we evaluate them using the dual descriptor (DD) $\Delta f(\vec{r})$,[85] a metric that allows the identification of nucleophilic and electrophilic sites.[86] We evaluate it as the difference between the corresponding Fukui functions (in the gas phase):

$$\Delta f(\vec{r}) = f^+(\vec{r}) - f^-(\vec{r}) \quad (7)$$

A (more) positive $\Delta f(\vec{r})$ indicates a (more) electrophilic region, and a (more) negative $\Delta f(\vec{r})$ indicates a (more) nucleophilic region. Positive (red) and negative (blue) DD isosurfaces are shown in Fig. 4a (isosurface values are provided in Table S6), indicating electrophilic and nucleophilic regions, respectively.

In $DFOB^-$, the boron atom appears strongly electrophilic, in agreement with the non-redox reactivity[87,88] of $DFOB^-$ with nucleophilic components of SEI, leading to a ring opening *via* attack on the boron atom. On the other hand, carbonyl oxygen atoms are the most nucleophilic, aligning with ring opening, induced by coordination of the Li^+ electrophile to carbonyl oxygen atoms.[89]

The nitrogen and sulphur atoms are nucleophilic and electrophilic centres of the $TFSI^-$ anion, respectively. The speciation of the $TFSI^-$ anion has been investigated *via* AIMD simulations for WiS electrolytes, revealing that the proton attaches to the nitrogen of $TFSI^-$, forming a superacid HTFSI,[90] in agreement with DD. An AIMD simulation of nucleophilic OH^- attack on $TFSI^-$ in the gas phase environment showed that OH^- preferentially attacks the sulphur atom.[91] However, simulations that explicitly include water solvent molecules indicated a preferential nucleophilic substitution at the carbon atom, driven by steric effects[91] that DD cannot capture. On the other hand, a nucleophilic attack of OH^- on the sulphur atom of $[MgTFSI]^+$ contact ion pair, explicitly solvated by diglyme, was also observed by AIMD, in line with DD.[92]

In TDI^-, the values of DD are rather low. The most electrophilic region appears to be the carbon atom of the cyano group,

Open Access Article. Published on 19 February 2026. Downloaded on 4/7/2026 12:08:39 AM. This article is licensed under a Creative Commons Attribution 3.0 Unported Licence.

Table 1 Condensed dual descriptor minima/maxima for TDI^-, $TFSI^-$, and $DFOB^-$ along with H^+/OH^- binding energies in the gas phase and in water (SMD)

	TDI^-	$TFSI^-$	$DFOB^-$
min CDD/e_0	−0.07	−0.22	−0.19
$\Delta E^{gas}_{H^+}$/eV	−12.33	−13.20	−12.96
$\Delta E^{SMD}_{H^+}$/eV	−11.09	−11.49	−11.38
max CDD/e_0	0.06	0.08	0.59
$\Delta E^{gas}_{OH^-}$/eV	2.23	2.31	1.53
$\Delta E^{SMD}_{OH^-}$/eV	−3.79	−3.42	−5.00

while the cyclic carbon atom, to which –CN is bonded, appears the most nucleophilic. This does not agree with the experimentally observed coordination of Li^+ and the proton of H_2O to the nitrogen atoms of TDI^- (cyano or cyclic).[93,94] We probe nucleophilicity of TDI^- sites by evaluating energetics for a model nucleophile (H^+), confirming the cyclic N atom as the most favourable site (Fig. S3). While DD successfully identified the most nucleophilic site it failed for the most electrophilic site, likely due to a low magnitude of DD and small variation in DD across the anion, possibly related to the strong chemical and thermal stability of LiTDI-containing electrolytes.[93,95]

Projection of DD values to specific atoms can be more useful, especially in the context of high-throughput approaches. We achieve this by partitioning the species charge into CM5 partial charges,[96] obtaining an atom-specific condensed dual descriptor (CDD). CDDs are illustrated in Fig. 4b, with the corresponding numerical values provided in Fig. S4. CDDs match the real-space DDs well and allow a direct comparison of reactive centres between the various anions: B of $DFOB^-$ stands out as a very strong electrophile, while N of $TFSI^-$ and carbonyl O of $DFOB^-$ are moderate nucleophiles. All other atoms exhibit significantly weaker electrophilicity/nucleophilicity.

To assess its predictive power, CDD is tested against the binding energies of anions with representative model species: electrophile H^+ and nucleophile OH^- (Table 1 and Fig. S3). We observe a linear correlation between the CDD maximum and H^+ binding energy, despite small energy differences between $TFSI^-$ and $DFOB^-$ (Fig. S4). While CDD fails to predict a slightly more favourable OH^- binding to TDI^- compared to $TFSI^-$, presumably due to the proximity of a strongly nucleophilic N, the strong nucleophilicity of the B atom of $DFOB^-$ with large CDD indeed leads to much stronger OH^- binding to $DFOB^-$ compared to both TDI^- and $TFSI^-$.

4. Conclusion

In conclusion, we have shown that descriptors from the framework of conceptual DFT can be used to understand the behavior of anions in battery electrolytes, including some important aspects of their (electro)chemical reactivity. While some descriptors are too simplistic to accurately predict all observables, they capture the key trends remarkably well, making them suitable for quick screening of the extensive chemical space, *e.g.*, for the initial layers of the computational funnel approach.[97] In addition to anions, the descriptors discussed in this work can be used to study solvent, diluent, and electrolyte additive molecules. More broadly, this framework could also be applied to other systems, where anions play a key role, such as electrolytes for Li-mediated nitrogen reduction reaction[98] or electrochemical CO_2 reduction.[99] We believe this work will motivate the community to utilize the variety of tools that conceptual DFT offers and accelerate the design of advanced electrolytes for electrochemical energy storage/conversion.

Author contributions

E. R. conceptualized the project, performed the calculations, and wrote the initial draft. E. R. and M. H. interpreted the data. M. H. supervised the project. R. D. secured funding and managed the project. All authors reviewed, edited, and approved the final version of the manuscript.

Conflicts of interest

There are no conflicts to declare.

Data availability

The data supporting this article have been included as part of the supplementary information (SI). Supplementary information: Cartesian coordinates of optimized molecular geometries. See DOI: https://doi.org/10.1039/d6ta00383d.

Acknowledgements

The research was funded by the Slovenian Research and Innovation Agency (ARIS) through core funding P2-0423 (E.R., R.D.) and P2-0152 (M.H.), and grants GC-0004 and J2-70085 (M.H.). The research was co-funded under the HyBReED project, supported by the European Union – NextGenerationEU. The authors acknowledge the HPC RIVR consortium and EuroHPC JU for funding this research by providing computing resources of the HPC system Vega at the Institute of Information Science, Maribor, Slovenia. The authors thank Alessandra Serva and Svit Menart for helpful discussions.

References

1 M. Armand and J.-M. Tarascon, Building better batteries, *Nature*, 2008, **451**, 652–657.
2 J. B. Goodenough and K.-S. Park, The Li-ion rechargeable battery: A perspective, *J. Am. Chem. Soc.*, 2013, **135**, 1167–1176.
3 L. Yang, N. M. Hagh, J. Roy, E. Macciomei, J. R. Klein, U. Janakiraman and M. E. Fortier, Review—challenges and opportunities in lithium metal battery technology, *J. Electrochem. Soc.*, 2024, **171**, 060504.
4 J. Xiang, Y. Wei, Y. Zhong, Y. Yang, H. Cheng, L. Yuan, H. Xu and Y. Huang, Building practical high-voltage cathode

Open Access Article. Published on 19 February 2026. Downloaded on 4/7/2026 12:08:39 AM. This article is licensed under a Creative Commons Attribution 3.0 Unported Licence.

materials for lithium-ion batteries, *Adv. Mater.*, 2022, **34**, 2200912.
5 L. Wang, Z. Wu, J. Zou, P. Gao, X. Niu, H. Li and L. Chen, Li-free cathode materials for high energy density lithium batteries, *Joule*, 2019, **3**, 2086–2102.
6 X. Fan and C. Wang, High-voltage liquid electrolytes for Li batteries: progress and perspectives, *Chem. Soc. Rev.*, 2021, **50**, 10486–10566.
7 M. Li, C. Wang, Z. Chen, K. Xu and J. Lu, New concepts in electrolytes, *Chem. Rev.*, 2020, **120**, 6783–6819.
8 L. Cheng, R. S. Assary, X. Qu, A. Jain, S. P. Ong, N. N. Rajput, K. Persson and L. A. Curtiss, Accelerating electrolyte discovery for energy storage with high-throughput screening, *J. Phys. Chem. Lett.*, 2015, **6**, 283–291.
9 X. Qu, A. Jain, N. N. Rajput, L. Cheng, Y. Zhang, S. P. Ong, M. Brafman, E. Maginn, L. A. Curtiss and K. A. Persson, The electrolyte genome project: A big data approach in battery materials discovery, *Comput. Mater. Sci.*, 2015, **103**, 56–67.
10 T. Mendez-Morales, Z. Li and M. Salanne, Computational screening of the physical properties of water-in-salt electrolytes, *Batter. Supercaps*, 2021, **4**, 646–652.
11 Y. Ko, M. A. Baird, X. Peng, T. Ogunfunmi, Y.-W. Byeon, L. M. Klivansky, H. Kim, M. C. Scott, J. Chen, A. J. D'Angelo, J. Chen, S. Sripad, V. Viswanathan and B. A. Helms, Omics-enabled understanding of electric aircraft battery electrolytes, *Joule*, 2024, **8**, 2393–2411.
12 S. C. Kim, S. T. Oyakhire, C. Athanitis, J. Wang, Z. Zhang, W. Zhang, D. T. Boyle, M. S. Kim, Z. Yu, X. Gao, T. Sogade, E. Wu, J. Qin, Z. Bao, S. F. Bent and Y. Cui, Data-driven electrolyte design for lithium metal anodes, *Proc. Natl. Acad. Sci. U. S. A*, 2023, **120**, e2214357120.
13 M. Zohair, V. Sharma, E. A. Soares, K. Nguyen, M. Giammona, L. Sundberg, A. Tek, E. A. V. Vital and Y.-H. La, Chemical foundation model-guided design of high ionic conductivity electrolyte formulations, *npj Comput. Mater.*, 2025, **11**, 283.
14 R. Atwi and N. N. Rajput, Guiding maps of solvents for lithium-sulfur batteries via a computational data-driven approach, *Patterns*, 2023, **4**, 100799.
15 D. Lu, R. Li, M. M. Rahman, P. Yu, L. Lv, S. Yang, Y. Huang, C. Sun, S. Zhang, H. Zhang, J. Zhang, X. Xiao, T. Deng, L. Fan, L. Chen, J. Wang, E. Hu, C. Wang and X. Fan, Ligand-channel-enabled ultrafast Li-ion conduction, *Nature*, 2024, **627**, 101–107.
16 R. Kumar, M. C. Vu, P. Ma and C. V. Amanchukwu, Electrolytomics: A unified big data approach for electrolyte design and discovery, *Chem. Mater.*, 2025, **37**, 2720–2734.
17 J. Ruža, P. Leon, K. Jun, J. Johnson, Y. Shao-Horn and R. Gómez-Bombarelli, Benchmarking classical molecular dynamics simulations for computational screening of lithium polymer electrolytes, *Macromolecules*, 2025, **58**, 6732–6742.
18 S. K. Kauwe, J. Graser, R. Murdock and T. D. Sparks, Can machine learning find extraordinary materials?, *Comput. Mater. Sci.*, 2020, **174**, 109498.
19 S. Ju, J. You, G. Kim, Y. Park, H. An and S. Han, Application of pretrained universal machine-learning interatomic potential for physicochemical simulation of liquid electrolytes in Li-ion batteries, *Digit. Discov.*, 2025, **4**, 1544–1559.
20 M. A. Makeev and N. N. Rajput, Computational screening of electrolyte materials: *status quo* and open problems, *Curr. Opin. Chem. Eng.*, 2019, **23**, 58–69.
21 P. Geerlings, F. De Proft and W. Langenaeker, Conceptual density functional theory, *Chem. Rev.*, 2003, **103**, 1793–1874.
22 D. Chakraborty and P. K. Chattaraj, Conceptual density functional theory based electronic structure principles, *Chem. Sci.*, 2021, **12**, 6264–6279.
23 L. R. Domingo, M. Ríos-Gutiérrez and P. Pérez, Applications of the conceptual density functional theory indices to organic chemistry reactivity, *Molecules*, 2016, **21**, 748.
24 E. Jónsson and P. Johansson, Electrochemical oxidation stability of anions for modern battery electrolytes: a CBS and DFT study, *Phys. Chem. Chem. Phys.*, 2015, **17**, 3697–3703.
25 P. Jankowski, M. Poterała, N. Lindahl, W. Wieczorek and P. Johansson, Chemically soft solid electrolyte interphase forming additives for lithium-ion batteries, *J. Mater. Chem. A*, 2018, **6**, 22609–22618.
26 A. Kopač Lautar, A. Hagopian and J.-S. Filhol, Modeling interfacial electrochemistry: concepts and tools, *Phys. Chem. Chem. Phys.*, 2020, **22**, 10569–10580.
27 A. Kopač Lautar, J. Bitenc, R. Dominko and J.-S. Filhol, Building *Ab Initio* interface Pourbaix diagrams to investigate electrolyte stability in the electrochemical double layer: Application to magnesium batteries, *ACS Appl. Mater. Interfaces*, 2021, **13**, 8263–8273.
28 L. H. B. Nguyen and J.-S. Filhol, Solvation–reduction coupling in Ca^{2+} electroactivity in glyme-based electrolytes: A first principles study, *Adv. Energy Mater.*, 2023, **13**, 2300311.
29 Y. Zhang, H. Zhuo, P. Lei, D. Tang, Q. Hu, X. Du, C.-J. Zheng, J.-L. Yang, Z.-Y. Gu, J. Zhao, S. Tao and X.-L. Wu, Fukui function-engineered gel electrolytes: Thermodynamic/kinetic-synergistic regulation for long-cycling zinc metal batteries, *Adv. Mater.*, 2025, **37**, 2508722.
30 S. Ilic, S. N. Lavan and J. G. Connell, Anion-derived contact ion pairing as a unifying principle for electrolyte design, *Chem*, 2024, **10**, 2987–3007.
31 X.-Q. Zhang, X. Chen, L.-P. Hou, B.-Q. Li, X.-B. Cheng, J.-Q. Huang and Q. Zhang, Regulating anions in the solvation sheath of lithium ions for stable lithium metal batteries, *ACS Energy Lett.*, 2019, **4**, 411–416.
32 Z. Huang, X. Li, Z. Chen, P. Li, X. Ji and C. Zhi, Anion chemistry in energy storage devices, *Nat. Rev. Chem.*, 2023, **7**, 616–631.
33 E. Rems, T. Šlosar, S. Drvarič Talian, M. Huš, R. Dominko and A. Serva, Strongly vs. weakly associating anions: transport–structure relationship in LiTFSI–$LiNO_3$ electrolytes, *Phys. Chem. Chem. Phys.*, 2025, **27**, 22082–22092.
34 J.-D. Chai and M. Head-Gordon, Long-range corrected hybrid density functionals with damped atom–atom

Open Access Article. Published on 19 February 2026. Downloaded on 4/7/2026 12:08:39 AM. This article is licensed under a Creative Commons Attribution 3.0 Unported Licence.

dispersion corrections, *Phys. Chem. Chem. Phys.*, 2008, **10**, 6615–6620.
35 F. Weigend and R. Ahlrichs, Balanced basis sets of split valence, triple zeta valence and quadruple zeta valence quality for H to Rn: Design and assessment of accuracy, *Phys. Chem. Chem. Phys.*, 2005, **7**, 3297–3305.
36 D. Rappoport and F. Furche, Property-optimized gaussian basis sets for molecular response calculations, *J. Chem. Phys.*, 2010, **133**, 134105.
37 F. Weigend, F. Furche and R. Ahlrichs, Gaussian basis sets of quadruple zeta valence quality for atoms H–Kr, *J. Chem. Phys.*, 2003, **119**, 12753–12762.
38 M. J. Frisch, G. W. Trucks, H. B. Schlegel, G. E. Scuseria, M. A. Robb, J. R. Cheeseman, G. Scalmani, V. Barone, G. A. Petersson, H. Nakatsuji, X. Li, M. Caricato, A. V. Marenich, J. Bloino, B. G. Janesko, R. Gomperts, B. Mennucci, H. P. Hratchian, J. V. Ortiz, A. F. Izmaylov, J. L. Sonnenberg, D. Williams-Young, F. Ding, F. Lipparini, F. Egidi, J. Goings, B. Peng, A. Petrone, T. Henderson, D. Ranasinghe, V. G. Zakrzewski, J. Gao, N. Rega, G. Zheng, W. Liang, M. Hada, M. Ehara, K. Toyota, R. Fukuda, J. Hasegawa, M. Ishida, T. Nakajima, Y. Honda, O. Kitao, H. Nakai, T. Vreven, K. Throssell, J. A. Montgomery Jr, J. E. Peralta, F. Ogliaro, M. J. Bearpark, J. J. Heyd, E. N. Brothers, K. N. Kudin, V. N. Staroverov, T. A. Keith, R. Kobayashi, J. Normand, K. Raghavachari, A. P. Rendell, J. C. Burant, S. S. Iyengar, J. Tomasi, M. Cossi, J. M. Millam, M. Klene, C. Adamo, R. Cammi, J. W. Ochterski, R. L. Martin, K. Morokuma, O. Farkas, J. B. Foresman, and D. J. Fox, "*Gaussian 16 Revision C.02*," , Gaussian, Inc., Wallingford CT, 2021.
39 B. P. Pritchard, D. Altarawy, B. Didier, T. D. Gibson and T. L. Windus, New basis set exchange: An open, up-to-date resource for the molecular sciences community, *J. Chem. Inf. Model.*, 2019, **59**, 4814–4820.
40 S. P. Ong, W. D. Richards, A. Jain, G. Hautier, M. Kocher, S. Cholia, D. Gunter, V. L. Chevrier, K. A. Persson and G. Ceder, Python materials genomics (pymatgen): A robust, open-source python library for materials analysis, *Comput. Mater. Sci.*, 2013, **68**, 314–319.
41 T. Lu, A comprehensive electron wavefunction analysis toolbox for chemists, Multiwfn, *J. Chem. Phys.*, 2024, **161**, 082503.
42 W. Humphrey, A. Dalke and K. Schulten, VMD: Visual molecular dynamics, *J. Mol. Graph.*, 1996, **14**, 33–38.
43 D. S. Hall, J. Self and J. R. Dahn, Dielectric constants for quantum chemistry and li-ion batteries: Solvent blends of ethylene carbonate and ethyl methyl carbonate, *J. Phys. Chem. C*, 2015, **119**, 22322–22330.
44 Y. Okamoto, *Ab Initio* calculations of thermal decomposition mechanism of $LiPF_6$-based electrolytes for lithium-ion batteries, *J. Electrochem. Soc.*, 2013, **160**, A404–A409.
45 T. Hou, K. D. Fong, J. Wang and K. A. Persson, The solvation structure, transport properties and reduction behavior of carbonate-based electrolytes of lithium-ion batteries, *Chem. Sci.*, 2021, **12**, 14740–14751.
46 A. Manthiram, An outlook on lithium ion battery technology, *ACS Cent. Sci.*, 2017, **3**, 1063–1069.
47 K. Xu, Electrolytes and interphases in Li-ion batteries and beyond, *Chem. Rev.*, 2014, **114**, 11503–11618.
48 S. A. Delp, O. Borodin, M. Olguin, C. G. Eisner, J. L. Allen and T. R. Jow, Importance of reduction and oxidation stability of high voltage electrolytes and additives, *Electrochim. Acta*, 2016, **209**, 498–510.
49 R. G. Parr and R. G. Pearson, Absolute hardness: companion parameter to absolute electronegativity, *J. Am. Chem. Soc.*, 1983, **105**, 7512–7516.
50 R. G. Pearson, Hard and soft acids and bases, *J. Am. Chem. Soc.*, 1963, **85**, 3533–3539.
51 J. Tomasi, B. Mennucci and R. Cammi, Quantum mechanical continuum solvation models, *Chem. Rev.*, 2005, **105**, 2999–3094.
52 A. V. Marenich, C. J. Cramer and D. G. Truhlar, Universal solvation model based on solute electron density and on a continuum model of the solvent defined by the bulk dielectric constant and atomic surface tensions, *J. Phys. Chem. B*, 2009, **113**, 6378–6396.
53 P. Jaramillo, P. Pérez, P. Fuentealba, S. Canuto and K. Coutinho, Solvent effects on global reactivity properties for neutral and charged systems using the sequential Monte Carlo quantum mechanics model, *J. Phys. Chem. B*, 2009, **113**, 4314–4322.
54 D. Strmcnik, I. E. Castelli, J. G. Connell, D. Haering, M. Zorko, P. Martins, P. P. Lopes, B. Genorio, T. Østergaard, H. A. Gasteiger, F. Maglia, B. K. Antonopoulos, V. R. Stamenkovic, J. Rossmeisl and N. M. Markovic, Electrocatalytic transformation of HF impurity to H_2 and LiF in lithium-ion batteries, *Nat. Catal.*, 2018, **1**, 255–262.
55 M. Martins, D. Haering, J. G. Connell, H. Wan, K. L. Svane, B. Genorio, P. Farinazzo Bergamo Dias Martins, P. P. Lopes, B. Gould, F. Maglia, R. Jung, V. Stamenkovic, I. E. Castelli, N. M. Markovic, J. Rossmeisl and D. Strmcnik, Role of catalytic conversions of ethylene carbonate, water, and HF in forming the solid-electrolyte interphase of Li-ion batteries, *ACS Catal.*, 2023, **13**, 9289–9301.
56 E. W. C. Spotte-Smith, T. B. Petrocelli, H. D. Patel, S. M. Blau and K. A. Persson, Elementary decomposition mechanisms of lithium hexafluorophosphate in battery electrolytes and interphases, *ACS Energy Lett.*, 2023, **8**, 347–355.
57 T. Kawamura, S. Okada and J. ichi Yamaki, Decomposition reaction of $LiPF_6$-based electrolytes for lithium ion cells, *J. Power Sources*, 2006, **156**, 547–554.
58 S. Trasatti, The absolute electrode potential: an explanatory note (recommendations 1986), *Pure Appl. Chem.*, 1986, **58**, 955–966.
59 N. N. Rajput, X. Qu, N. Sa, A. K. Burrell and K. A. Persson, The coupling between stability and ion pair formation in magnesium electrolytes from first-principles quantum mechanics and classical molecular dynamics, *J. Am. Chem. Soc.*, 2015, **137**, 3411–3420.

 This journal is © The Royal Society of Chemistry 2026

Open Access Article. Published on 19 February 2026. Downloaded on 4/7/2026 12:08:39 AM. This article is licensed under a Creative Commons Attribution 3.0 Unported Licence.

60 E. R. Fadel, F. Faglioni, G. Samsonidze, N. Molinari, B. V. Merinov, W. A. Goddard III, J. C. Grossman, J. P. Mailoa and B. Kozinsky, Role of solvent-anion charge transfer in oxidative degradation of battery electrolytes, *Nat. Commun.*, 2019, **10**, 3360.

61 E. Peled, D. Golodnitsky and G. Ardel, Advanced model for solid electrolyte interphase electrodes in liquid and polymer electrolytes, *J. Electrochem. Soc.*, 1997, **144**, L208.

62 S. A. Krachkovskiy, J. D. Bazak, S. Fraser, I. C. Halalay and G. R. Goward, Determination of mass transfer parameters and ionic association of $LiPF_6$: Organic carbonates solutions, *J. Electrochem. Soc.*, 2017, **164**, A912.

63 O. Borodin, J. Self, K. A. Persson, C. Wang and K. Xu, Uncharted waters: Super-concentrated electrolytes, *Joule*, 2020, **4**, 69–100.

64 H. Wang, Z. Yu, X. Kong, S. C. Kim, D. T. Boyle, J. Qin, Z. Bao and Y. Cui, Liquid electrolyte: The nexus of practical lithium metal batteries, *Joule*, 2022, **6**, 588–616.

65 R. G. Parr and W. Yang, Density functional approach to the frontier-electron theory of chemical reactivity, *J. Am. Chem. Soc.*, 1984, **106**, 4049–4050.

66 J. P. Perdew, R. G. Parr, M. Levy and J. L. Balduz, Density-functional theory for fractional particle number: Derivative discontinuities of the energy, *Phys. Rev. Lett.*, 1982, **49**, 1691–1694.

67 H. Gao, F. Maglia, P. Lamp, K. Amine and Z. Chen, Mechanistic study of electrolyte additives to stabilize high-voltage cathode–electrolyte interface in lithium-ion batteries, *ACS Appl. Mater. Interfaces*, 2017, **9**, 44542–44549.

68 B. Wang, J. Wang, L. Zhang, P. K. Chu, X.-F. Yu, R. He and S. Bian, Adsorptive shield derived cathode electrolyte interphase formation with impregnation on $LiNi_{0.8}Mn_{0.1}Co_{0.1}O_2$ cathode: A mechanism-guiding-experiment study, *ACS Appl. Mater. Interfaces*, 2024, **16**, 50747–50756.

69 Y. Zhu, Y. Li, M. Bettge and D. P. Abraham, Positive electrode passivation by LiDFOB electrolyte additive in high-capacity lithium-ion cells, *J. Electrochem. Soc.*, 2012, **159**, A2109.

70 I. A. Shkrob, Y. Zhu, T. W. Marin and D. P. Abraham, Mechanistic insight into the protective action of bis(oxalato)borate and difluoro(oxalate)borate anions in li-ion batteries, *J. Phys. Chem. C*, 2013, **117**, 23750–23756.

71 M. Mao, B. Huang, Q. Li, C. Wang, Y.-B. He and F. Kang, *In-situ* construction of hierarchical cathode electrolyte interphase for high performance $LiNi_{0.8}Co_{0.1}Mn_{0.1}O_2$/Li metal battery, *Nano Energy*, 2020, **78**, 105282.

72 S. Jiao, X. Ren, R. Cao, M. H. Engelhard, Y. Liu, D. Hu, D. Mei, J. Zheng, W. Zhao, Q. Li, N. Liu, B. D. Adams, C. Ma, J. Liu, J.-G. Zhang and W. Xu, Stable cycling of high-voltage lithium metal batteries in ether electrolytes, *Nat. Energy*, 2018, **3**, 739–746.

73 E. K. W. Andersson, L.-T. Wu, L. Bertoli, Y.-C. Weng, D. Friesen, K. Elbouazzaoui, S. Bloch, R. Ovsyannikov, E. Giangrisostomi, D. Brandell, J. Mindemark, J.-C. Jiang and M. Hahlin, Initial SEI formation in LiBOB-, LiDFOB- and $LiBF_4$-containing PEO electrolytes, *J. Mater. Chem. A*, 2024, **12**, 9184–9199.

74 J. Holoubek, Q. Yan, H. Liu, E. J. Hopkins, Z. Wu, S. Yu, J. Luo, T. A. Pascal, Z. Chen and P. Liu, Oxidative stabilization of dilute ether electrolytes via anion modification, *ACS Energy Lett.*, 2022, **7**, 675–682.

75 M. Paillot, A. Wong, S. A. Denisov, P. Soudan, P. Poizot, B. Montigny, M. Mostafavi, M. Gauthier and S. Le Caër, Predicting degradation mechanisms in lithium bistriflimide "water-in-salt" electrolytes for aqueous batteries, *ChemSusChem*, 2023, **16**, e202300692.

76 P. C. Howlett, E. I. Izgorodina, M. Forsyth and D. R. MacFarlane, Electrochemistry at negative potentials in bis(trifluoromethanesulfonyl)amide ionic liquids, *Z. Phys. Chem.*, 2006, **220**, 1483–1498.

77 K. Forster-Tonigold, F. Buchner, A. Groß and R. J. Behm, Reactive interactions between the ionic liquid BMP-TFSI and a Na surface, *Batter. Supercaps*, 2023, **6**, e202300336.

78 J. Alvarado, M. A. Schroeder, T. P. Pollard, X. Wang, J. Z. Lee, M. Zhang, T. Wynn, M. Ding, O. Borodin, Y. S. Meng and K. Xu, Bisalt ether electrolytes: a pathway towards lithium metal batteries with Ni-rich cathodes, *Energy Environ. Sci.*, 2019, **12**, 780–794.

79 H.-G. Steinrück, C. Cao, M. R. Lukatskaya, C. J. Takacs, G. Wan, D. G. Mackanic, Y. Tsao, J. Zhao, B. A. Helms, K. Xu, O. Borodin, J. F. Wishart and M. F. Toney, Interfacial speciation determines interfacial chemistry: X-ray-induced lithium fluoride formation from water-in-salt electrolytes on solid surfaces, *Angew. Chem., Int. Ed.*, 2020, **59**, 23180–23187.

80 I. A. Shkrob, K. Z. Pupek, J. A. Gilbert, S. E. Trask and D. P. Abraham, Chemical stability of lithium 2-trifluoromethyl-4,5-dicyanoimidazolide, an electrolyte salt for Li-ion cells, *J. Phys. Chem. C*, 2016, **120**, 28463–28471.

81 F. Lindgren, C. Xu, J. Maibach, A. M. Andersson, M. Marcinek, L. Niedzicki, T. Gustafsson, F. Björefors and K. Edström, A hard X-ray photoelectron spectroscopy study on the solid electrolyte interphase of a lithium 4,5-dicyano-2-(trifluoromethyl)imidazolide based electrolyte for Si-electrodes, *J. Power Sources*, 2016, **301**, 105–112.

82 T. Stuyver, F. De Proft, P. Geerlings and S. Shaik, How do local reactivity descriptors shape the potential energy surface associated with chemical reactions? The valence bond delocalization perspective, *J. Am. Chem. Soc.*, 2020, **142**, 10102–10113.

83 B. Wang, P. Geerlings, S. Liu and F. De Proft, Extending the scope of conceptual density functional theory with second order analytical methodologies, *J. Chem. Theory Comput.*, 2024, **20**, 1169–1184.

84 S. Ilic, M. Martins, H. Liu, P. Farinazzo Bergamo Dias Martins, D. Haering, J. Yang, T. Hatsukade, B. Genorio, S. E. Weitzner, L. F. Wan, Z. Zhang, J. G. Connell, B. Key, J. Cabana and D. Strmcnik, An unwanted guest in the electrochemical oxidation of high-voltage Li-ion battery electrolytes: the life of highly reactive protons, *Energy Environ. Sci.*, 2025, **18**, 8303–8312.

85 C. Morell, A. Grand and A. Toro-Labbé, New dual descriptor for chemical reactivity, *J. Phys. Chem. A*, 2005, **109**, 205–212.

Open Access Article. Published on 19 February 2026. Downloaded on 4/7/2026 12:08:39 AM.
This article is licensed under a Creative Commons Attribution 3.0 Unported Licence.

86 J. I. Martínez-Araya, Why is the dual descriptor a more accurate local reactivity descriptor than fukui functions?, *J. Math. Chem.*, 2014, **53**, 451–465.
87 S. Shui Zhang, An unique lithium salt for the improved electrolyte of Li-ion battery, *Electrochem. Commun.*, 2006, **8**, 1423–1428.
88 T. Schedlbauer, S. Krüger, R. Schmitz, R. Schmitz, C. Schreiner, H. Gores, S. Passerini and M. Winter, Lithium difluoro(oxalato)borate: A promising salt for lithium metal based secondary batteries?, *Electrochim. Acta*, 2013, **92**, 102–107.
89 M. Xu, L. Zhou, L. Hao, L. Xing, W. Li and B. L. Lucht, Investigation and application of lithium difluoro(oxalate) borate (LiDFOB) as additive to improve the thermal stability of electrolyte for lithium-ion batteries, *J. Power Sources*, 2011, **196**, 6794–6801.
90 K. Goloviznina, A. Serva and M. Salanne, Speciation of the proton in water-in-salt electrolytes, *Faraday Discuss.*, 2024, **253**, 478–492.
91 A. France-Lanord, F. Pietrucci, A. M. Saitta, J.-M. Tarascon, A. Grimaud and M. Salanne, Chemical decomposition of the TFSI anion under aqueous basic conditions, *PRX Energy*, 2022, **1**, 013005.
92 Y. Yu, A. Baskin, C. Valero-Vidal, N. T. Hahn, Q. Liu, K. R. Zavadil, B. W. Eichhorn, D. Prendergast and E. J. Crumlin, Instability at the electrode/electrolyte interface induced by hard cation chelation and nucleophilic attack, *Chem. Mater.*, 2017, **29**, 8504–8512.
93 C. Xu, S. Renault, M. Ebadi, Z. Wang, E. Björklund, D. Guyomard, D. Brandell, K. Edström and T. Gustafsson, LiTDI: A highly efficient additive for electrolyte stabilization in lithium-ion batteries, *Chem. Mater.*, 2017, **29**, 2254–2263.
94 M. Dranka, P. Jankowski and G. Z. Żukowska, Snapshots of the hydrolysis of lithium 4,5-dicyanoimidazolate–glyme solvates. impact of water molecules on aggregation processes in lithium-ion battery electrolytes, *J. Phys. Chem. C*, 2018, **122**, 3201–3210.
95 L. Niedzicki, E. Karpierz, A. Bitner, M. Kasprzyk, G. Zukowska, M. Marcinek and W. Wieczorek, Optimization of the lithium-ion cell electrolyte composition through the use of the LiTDI salt, *Electrochim. Acta*, 2014, **117**, 224–229.
96 A. V. Marenich, S. V. Jerome, C. J. Cramer and D. G. Truhlar, Charge model 5: An extension of Hirshfeld population analysis for the accurate description of molecular interactions in gaseous and condensed phases, *J. Chem. Theory Comput.*, 2012, **8**, 527–541.
97 A. Benayad, D. Diddens, A. Heuer, A. N. Krishnamoorthy, M. Maiti, F. L. Cras, M. Legallais, F. Rahmanian, Y. Shin, H. Stein, M. Winter, C. Wölke, P. Yan and I. Cekic-Laskovic, High-throughput experimentation and computational freeway lanes for accelerated battery electrolyte and interface development research, *Adv. Energy Mater.*, 2022, **12**, 2102678.
98 X. Fu, S. Li, N. H. Deissler, J. B. V. Mygind, J. Kibsgaard and I. Chorkendorff, Effect of lithium salt on lithium-mediated ammonia synthesis, *ACS Energy Lett.*, 2024, **9**, 3790–3795.
99 K. Trapp, J. Yoo and M. R. Lukatskaya, The role of anions and additives in electrochemical CO_2 reduction, *Curr. Opin. Electrochem.*, 2025, **52**, 101707.

 This journal is © The Royal Society of Chemistry 2026